

A Tutorial on Time-Evolving Dynamical Bayesian Inference

Tomislav Stankovski¹, Andrea Duggento², Peter V. E. McClintock¹, and Aneta Stefanovska^{1*}

¹ Department of Physics, Lancaster University, Lancaster, LA1 4YB, United Kingdom and

² Medical Physics Section, Faculty of Medicine, Tor Vergata University, Rome, Italy

We present a tutorial for Bayesian inference of time-evolving coupled systems in the presence of noise. It includes the necessary theoretical description and the algorithms for its implementation. For general programming purposes, a pseudocode description is given. Examples based on coupled phase and limit-cycle oscillators illustrate the most important features. Codes written in MatLab for the method and the examples accompany the tutorial.

I. INTRODUCTION

The Bayesian methods for dynamical inference make for important signal processing techniques. Their applications include physics, biology and communications. Theoretical studies of such methods have already been presented extensively [1–5]. Of particular interest is the method [1, 2] published recently, which can identify time-evolving coupled dynamics and is able to follow the time-variability of coupling functions. Here we discuss how this method can be implemented, including the algorithms, programming and applications. The problems and phenomena that are treated by the method are already relatively complex, hence in order to make the presentation more understandable we provide a different presentation style with examples that are simple and elementary.

The tutorial is organized as follows. First, in section II we present the theoretical terms needed for the implementation of Bayesian inference. The algorithms and the programming description are given in section III. Application of the method on two examples is shown in section IV. The first example uses coupled phase oscillators to present the basics of the inference of time-evolving phase dynamics in presence of noise. The second example uses coupled limit-cycle oscillators, presenting also the reconstruction and detection of synchronization and coupling functions. Some important generalizations of the framework are presented in section V. Finally, short concluding remarks are given in section VI.

II. INFERENCE IMPLEMENTATION

Given that l vectors of N -samples time-series $\mathcal{X} = \{\phi_{l,n} \equiv \phi_l(t_n)\}$ ($t_n = nh$) are provided, the main task for the method

is to infer the unknown model parameters and the noise diffusion matrix $\mathcal{M} = \{c_k^{(l)}, E_{ij}, \}\}$. The model for the interacting phase dynamics to be inferred (e.g. for $l = 2$ oscillators) is given by the following stochastic differential equations:

$$\dot{\phi}_l = \sum_{k=-K}^K c_k^{(l)} \Phi_{l,k}(\phi_1, \phi_2) + \xi_l(t), \quad (1)$$

where $\Phi_{1,0} = \Phi_{2,0} = 1$, $c_0^{(l)} = \omega_l$ are the respective frequencies, and the rest of $\Phi_{l,k}$ and $c_k^{(l)}$ are the K most important Fourier components which serve as base functions for the inference. The noise is assumed to be white, Gaussian, and parameterized by a noise diffusion matrix (\mathbf{E} 2×2): $\langle \xi_i(t) \xi_j(\tau) \rangle = \delta(t - \tau) E_{ij}$.

The inference exploits Bayes' theorem, assumes Euler midpoint discretisation $[\phi_{l,n} = (\phi_{l,n+1} - \phi_{l,n})/h$ and $\phi_{l,n}^* = (\phi_{l,n} + \phi_{l,n+1})/2$], and uses the properties of the stochastic integral to evaluate the likelihood function (see [1–5] for details). Assuming that the parameters \mathbf{c} have a multivariate normal distribution, with mean $\bar{\mathbf{c}}$, and a covariance matrix $\Sigma \equiv \Xi^{-1}$, the stationary distribution is calculated recursively using only four equations: for the parameters \mathbf{c} , for the noise matrix \mathbf{E} , for the concentration matrix Ξ and for temporary equation \mathbf{r} , which will be defined below. These four equations are applied on every time-series window, and they are central for the implementation of the inference. For easier implementation, and as an alternative to the theoretical presentation [1, 2], in the following we present the matrix notation of these equations.

For sake of clarification, ignoring the stochastic term, we can write Eq.1 at every point in time t_n in matrix form:

$$\begin{bmatrix} \dot{\phi}_{1,n} \\ \vdots \\ \dot{\phi}_{l,n} \end{bmatrix} = \begin{bmatrix} \Phi_{1,1}(\phi_{1,n}^*) & \dots & 0 \\ \vdots & \ddots & \vdots \\ 0 & \dots & \Phi_{l,1}(\phi_{1,n}^*) \end{bmatrix} \dots \begin{bmatrix} \Phi_{1,K}(\phi_{1,n}^*) & \dots & 0 \\ \vdots & \ddots & \vdots \\ 0 & \dots & \Phi_{l,K}(\phi_{1,n}^*) \end{bmatrix} \times \begin{bmatrix} c_1^{(1)} \\ \vdots \\ c_1^{(l)} \\ \vdots \\ c_K^{(1)} \\ \vdots \\ c_K^{(l)} \end{bmatrix}$$

The big matrix in the center can be seen as composed by K blocks of diagonal l -sized matrices. We can define the latter matrix multiplication as:

$$\dot{\phi}(t_n) = \mathbf{P}(t_n) \times \mathbf{c}. \quad (2)$$

From Eq. (2) and the discussion in [3], the noise matrix \mathbf{E} can be expressed as:

$$\mathbf{E} = \frac{h}{N} \sum_{n=1}^N \left(\dot{\phi}(t_n) - \mathbf{P}(t_n) \mathbf{c} \right)^T \left(\dot{\phi}(t_n) - \mathbf{P}(t_n) \mathbf{c} \right). \quad (3)$$

Next, the equation for the concentration matrix Ξ (i.e. the inverse of the covariance matrix Σ) can be calculated as:

$$\Xi = \Xi_{\text{prior}} + h \sum_{n=1}^N \mathbf{P}(t_n)^T \mathbf{E}^{-1} \mathbf{P}(t_n). \quad (4)$$

Note that, while more compact, we do not suggest that the matrix notation should be implemented as it is because the matrix \mathbf{P} is mostly filled with zeros and such implementation might produce very inefficient code. Similarly, one can express the temporary matrix variable \mathbf{r} :

$$\mathbf{r} = \Xi_{\text{prior}} \mathbf{c} + h \sum_{n=0}^N \mathbf{P}(t_n)^T \mathbf{E}^{-1} \dot{\phi}(t_n) - \frac{h}{2} \sum_{n=0}^N \mathbf{v}(t_n), \quad (5)$$

where each element on the lines of the vector $\mathbf{v}(t_n) = \frac{\partial \Phi_{l,k}(\phi_{l,n})}{\partial \phi_l}$ is, in practice, the elements of each column of $\mathbf{P}(t_n)$ derived with respect of the l -th variable, where l is the corresponding line of the element of $\mathbf{P}(t_n)$.

Finally, after the results from the other calculations the parameters vector \mathbf{c} is evaluated as:

$$\mathbf{c} = \Xi^{-1} \mathbf{r}. \quad (6)$$

By evaluating the four equations (3)-(6) using the readout time series $\mathcal{X} = \{\phi_{l,n} \equiv \phi_l(t_n)\}$ one can effectively calculate the multivariate probability $\mathcal{N}_{\mathcal{X}}(\mathbf{c}|, \bar{\mathbf{c}}, \Xi)$ which explicitly defines the probability density of each parameter set of the dynamical system. Following the matrix notation and the respective dimensions, one can implement the method consistently. For example, if we are given two phase time-series ($l = 2$) and we use six base functions in total ($K = 6$), then the respective dimensions of the matrices are: $\mathbf{E}_{l \times l} = \mathbf{E}_{2 \times 2}$, $\mathbf{r}_{K \times 1} = \mathbf{r}_{6 \times 1}$, $\Xi_{K \times K} = \Xi_{6 \times 6}$, $\mathbf{c}_{1 \times K} = \mathbf{c}_{1 \times 6}$, $\mathbf{P}_{l \times K} = \mathbf{P}_{2 \times 6}$ and $\mathbf{v}_{K \times 1} = \mathbf{v}_{6 \times 1}$.

The inference method needs to follow the time-evolution of the parameter set \mathbf{c} while separating the effects from the noise. In order to achieve this we modify the propagation procedure between the covariance of the current posterior Σ_{post} and the next prior $\Sigma_{\text{prior}}^{n+1}$ [1]. The definite matrix Σ_{diff} is introduced and shows how much each parameter diffuses normally. Thus, the next prior probability of the parameters is the convolution of two current normal multivariate distributions, Σ_{post} and Σ_{diff} : $\Sigma_{\text{prior}}^{n+1} = \Sigma_{\text{post}}^n + \Sigma_{\text{diff}}^n$. We consider Σ_{diff} to be such that there is no change of correlation between parameters ($\rho_{ij} = \delta_{ij}$) and that each standard deviation σ_i is a known

fraction of the relevant standard deviation from the posterior covariance (or parameters) $\sigma_i = p_w(\sigma_{\text{post}}^n)_i$, where p_w is a constant parameter. In practice this means that Σ_{diff} has zero values everywhere, except for the diagonal values, which are a fraction of the diagonal values of the posterior Σ_{post} .

III. ALGORITHMS AND PROGRAMMING

In this section we discuss the algorithmic and programming details for the implementation. First we present arguably the most complicated part; the algorithm for the dynamical Bayesian inference applied on a single window of readout data. The algorithm employing recursion using the Eqs. (3)-(6) can be summarized with the following steps:

- i) the algorithm starts from a $\mathbf{c}_{\text{prior}}$ and Ξ_{prior} ,
- ii) noise matrix \mathbf{E}_{new} is calculated using Eq. (3),
- iii) Ξ_{new} is calculated using Eq. (4),
- iv) \mathbf{r} is calculated using Eq. (5),
- v) \mathbf{c}_{new} is calculated using Eq. (6),
- vi) then again to point ii) using \mathbf{c}_{new} as \mathbf{c} .

The stopping rule is when a ‘convergence’ is reached i.e. when further running the algorithm would not modify \mathbf{c} and Ξ any further. For example, we used the condition: $\sum (\mathbf{c}_{\text{old}} - \mathbf{c}_{\text{new}})^2 / \mathbf{c}_{\text{new}}^2 < \epsilon$ where ϵ is some very small constant. Since the problem is parabolic, this convergence is very fast – typically a few cycles [27]. The prior distribution is assumed to be a noninformative “flat” acting as an initial limit of an infinitely large normal distribution, by setting $\Xi_{\text{prior}} = 0$ and $\mathbf{c}_{\text{prior}} = 0$.

For general programming purposes, in the following we outline an informal pseudo-code description of the main algorithms and sub-algorithms. The comments are presented in grey. First we describe the algorithm for the Bayesian inference:

Algorithm 1: Bayesian inference

```
\backslash\ calculate temporary variables beforehand
FOR k=1:N
    - calculate P
    - calculate v
    FOR i=1:k
        FOR j=1:k
            hPTP(i,j)=hPTP(i,j)+P(i mod l, i div l)*P(j mod l, j div l)
        ENDFOR
        FOR g=1:l
            hPtx(i,g)=hPtx(i,g)+P(i mod l, i div l)*\dot{\phi}_g(k)
        ENDFOR
    ENDFOR
    hV2=hV2+v
ENDFOR
hPtx=h*hPtx; hPTP=h*hPTP; hV2=0.5*h*hV2
```

```

 $c_{pt} = c_{pr}$ 
FOR lp=1:MaxLoops  \\main recursive loop
  - calculate  $\mathbf{E}$ 
  - calculate  $c_{pt}$ 
  IF SUM( $(c_{pr} - c_{pt})^2 / c_{pt}^2$ ) < SmallError
    RETURN
  ENDIF
   $c_{pr} = c_{pt}$ 
ENDFOR

```

The standard functions *mod* and *div* are used only to position the calculation on the right indexes. Since indexes can have different notations in various programming languages (i.e. starting from zero $i = 0, 1, \dots$ or one $i = 1, 2, \dots$), one should take care when applying *mod* and *div* in this context. The sub-algorithms ‘calculate P ’ and ‘calculate v ’ depend on the particular base functions and their partial derivatives. They only involve a simply evaluation of the base functions in respect to $\phi^*(k)$, and will not be discussed in detail. The other main calculations are performed within ‘calculate \mathbf{E} ’ and ‘calculate c_{pt} ’, which are discussed in detail bellow.

Algorithm 2: **calculate \mathbf{E}** \\use of Eq. (3)

```

FOR i=1:N
  - calculate  $\mathbf{P}$ 
   $\mathbf{E} = \mathbf{E} + (\dot{\phi}_i \mathbf{P}^* \mathbf{c}) * (\text{transpose of } (\dot{\phi}_i \mathbf{P}^* \mathbf{c}))$  \\where  $\dot{\phi}_{2 \times N}$ 
ENDFOR
 $\mathbf{E} = h/N * \mathbf{E}$ 

```

Finally, the algorithm for calculation of the parameters is expressed as:

Algorithm 3: **calculate \mathbf{c}**

$\text{invE} = \text{inverse of } \mathbf{E}$

```

\\calculate  $\mathbf{\Xi}$ , Eq. (4)
FOR i=1:K
  FOR j=1:K
     $\mathbf{\Xi}_{pt}(i,j) = h \text{PTP}(i,j) * \text{invE}(i \text{ mod } l, j \text{ mod } l)$ 
  ENDFOR
ENDFOR
 $\mathbf{\Xi}_{pt} = \mathbf{\Xi}_{pr} + \mathbf{\Xi}_{pt}$ 

\\calculate  $\mathbf{r}$ , Eq. (5)
FOR i=1:K
  FOR j=1:l
     $\mathbf{r}(i) = \mathbf{r}(i) + h \text{Ptx}(i,j) * \text{invE}(i \text{ mod } l, j)$ 
  ENDFOR
ENDFOR
 $\mathbf{r} = \mathbf{\Xi}_{pr} * \mathbf{c} + \mathbf{r} + h \mathbf{V2}$ 

\\calculate  $\mathbf{c}$ , Eq. (6)
 $\mathbf{c} = (\text{inverse of } \mathbf{\Xi}_{pt}) * \mathbf{r}$ 

```

The three described algorithms are applied to a single window of data. The time-series are separated into sequential blocks of data and the algorithms are applied to each of them. The core of Bayesian inference is that the evaluation of the next block of data depends and uses the results of the evaluation from the previous block. The process of information propagation, between the posterior and the next prior distribution, can be adjusted to allow the time-variability of the parameters to be followed. We used propagation depending on the concentration matrix $\mathbf{\Xi}_{pt}$ or the parameters vector \mathbf{c}_{pt} . In the following we describe the propagation with respect to the concentration matrix $\mathbf{\Xi}_{pt}$:

Algorithm 4: **Propagation**

$\text{invE}^n = \text{inverse of } \mathbf{\Xi}_{pt}^n$;

$\text{invDiff}^n = 0$

FOR i=1:K

$\text{invDiff}^n(i,i) = p_w^2 * \text{invE}^n(i,i)$

ENDFOR

$\mathbf{\Xi}_{pt}^{n+1} = \text{inverse of } (\text{invDiff}^n + \text{invE}^n)$

Once the inference is performed, one can use the inferred parameters to detect certain dynamical and phenomenological characteristics of the interacting systems. For example, calculating the norm of the parameters which are inferred with the relevant base functions one can detect the coupling strength and directionality between the oscillators [6–10]. Similarly, one can reconstruct the form of the coupling function [1, 11–14]. To evaluate if the systems are synchronized, one can test if systems with such inferred parameters are undergoing synchronization [15–17]. This can be done, for example, with maps representation and the modified Newton root-finding method (see [2] for details).

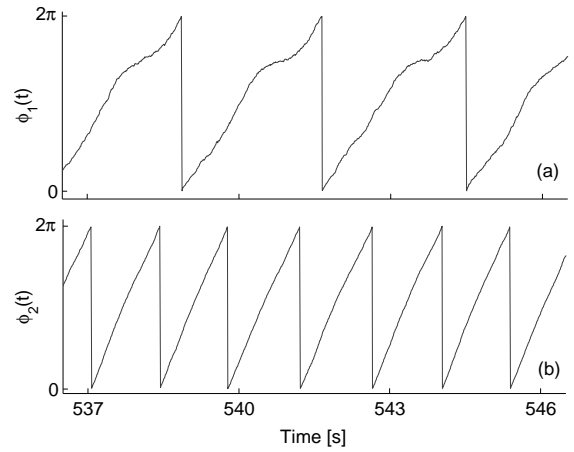


Figure 1: The instantaneous phases generated by the model of two coupled phase oscillators (7). (a) presents the phase from ϕ_1 and (b) from ϕ_2 . For simpler presentation, the phases are ‘wrapped’ in 2π .

IV. EXAMPLES

This section outlines two examples for phase reconstruction of coupled oscillators with time-varying dynamics and subject to noise. The first example illustrates the basics of the inference on a simple phase oscillators model, while the second example involves limit-cycle oscillators and presents the detection of several characteristics and relationships that can be detected from the inferred parameters. MatLab codes for the examples are provided at [28].

A. Coupled phase oscillators

In order to present in a transparent way the basics of the inference technique we first consider two coupled phase oscillators [18] subject to noise:

$$\begin{aligned}\dot{\phi}_1 &= \omega_1(t) + a_1 \sin(\phi_1) + a_3(t) \sin(\phi_2) + \xi_1(t) \\ \dot{\phi}_2 &= \omega_2 + a_2 \sin(\phi_1) + a_4 \sin(\phi_2) + \xi_2(t).\end{aligned}\quad (7)$$

Each oscillator is described by the frequency parameter ω_1 , ω_2 , the parameters for the self dynamics a_1, a_4 and the coupling parameters a_2, a_3 for the direct influence from the other oscillator. Two parameters are set to be periodically time-varying, the frequency $\omega_1(t) = 2 - 0.5 \sin(2\pi 0.00151t)$ and the coupling parameter $a_3(t) = 0.8 - 0.3 \sin(2\pi 0.0012t)$. The noises are set to be white Gaussian and uncorrelated between themselves. The rest of the parameters are $\omega_2 = 4.53$, $a_1 = 0.8$, $a_2 = 0$, $a_4 = 0.6$, $E_{11} = 0.03$ and $E_{22} = 0.01$. Fig. 1 shows the nature and the noise perturbations of the instantaneous phases on which the Bayesian inference is applied.

The choice to use phase oscillators is very convenient for the inference because one needs to reconstruct the same phase dynamics. Therefore, the phase model is known beforehand and the deterministic terms of the *rhs* of coupled system (7) are the actual base functions to be used in order to infer the six parameters ($\omega_1, \omega_2, a_1, a_2, a_3$ and a_4). The results from the inference of one block of data are presented in Table IV. One can notice that the method reconstructs the intrinsic parameters successfully and with high precision. Additionally, and this is unique for this method, the level and the correlations of the noise are inferred very precisely. Fig. 2 shows the time-variations of all the parameters inferred from sequential windows of length $w = 40$ s, and propagation constant $p_w = 0.2$. It is easy to notice that the parameters and their time-variability are precisely inferred.

B. Coupled limit-cycle oscillators

The second example involves a system of two coupled limit-cycle oscillators, which can serve as a model for a number of oscillating processes in nature, including cardio-respiratory, electrochemical, mechanical, biological [1, 14, 19, 20]. The model consists of two interacting Poincaré oscillators subject to noise:

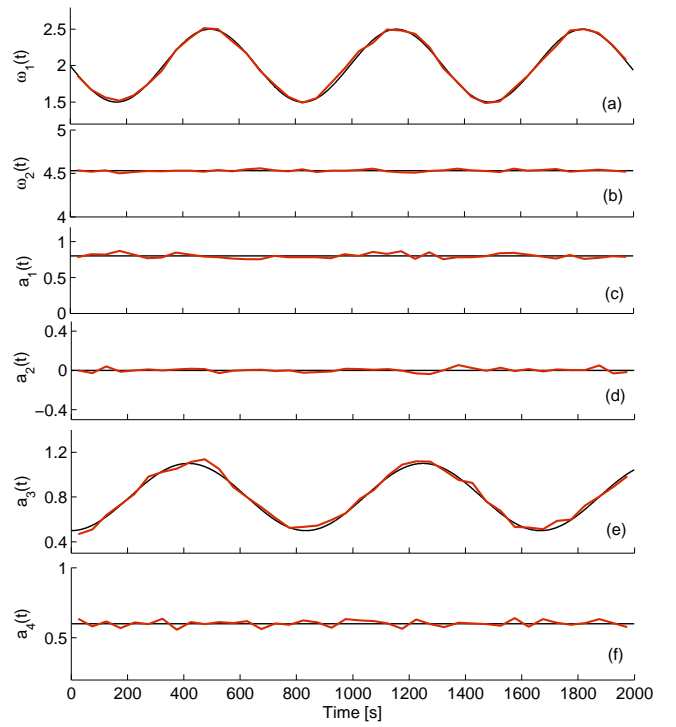


Figure 2: Time-evolution of the inferred parameters from model (7). (a) and (b) present the two frequencies, (c) and (f) the self dynamics parameters, and (d) and (e) present the coupling parameters. The original intrinsic values of the parameters are presented with black color, underneath the inferred parameters.

$$\begin{aligned}\dot{x}_1 &= -\left(\sqrt{x_1^2 + y_1^2} - 1\right)x_1 - \omega_1(t)y_1 + \varepsilon_1(x_2 - x_1) + \xi_1(t) \\ \dot{y}_1 &= -\left(\sqrt{x_1^2 + y_1^2} - 1\right)y_1 + \omega_1(t)x_1 + \varepsilon_1(y_2 - y_1) + \xi_2(t)\end{aligned}$$

$$\begin{aligned}\dot{x}_2 &= -\left(\sqrt{x_2^2 + y_2^2} - 1\right)x_2 - \omega_2 y_2 + \varepsilon_2(t)(x_1 - x_2) + \xi_3(t) \\ \dot{y}_2 &= -\left(\sqrt{x_2^2 + y_2^2} - 1\right)y_2 + \omega_2 x_2 + \varepsilon_2(t)(y_1 - y_2) + \xi_4(t),\end{aligned}\quad (8)$$

where periodic time-variability is introduced in the frequency of the first oscillator $\omega_1(t) = 1 - 0.4 \sin(2\pi 0.002t)$ and the coupling parameter from the first to the second oscillator $\varepsilon_2(t) = 0.2 - 0.1 \sin(2\pi 0.0017t)$. The noises are white Gaussian again, with no correlations between them. The rest of the parameters are $\omega_2 = 4.91$, $\varepsilon_1 = 0.05$, $E_{11} = E_{22} = 0.007$ and $E_{33} = E_{44} = 0.004$. The systems are simulated in state space, and the corresponding signals and phase portrait of the first system are given in Fig. 3 (a) and (b).

The phases are estimated as $\phi_i = \arctan(y_i/x_i)$ (arctan being a four-quadrant function) from the state signals. Alternatively, one can use Hilbert [20] or synchrosqueezed transform [21]. The choice of base functions for the inference needs to be determined so that the phase dynamics can be

Parameters	ω_1	ω_2	a_1	a_2	a_3	a_4	E_{11}	E_{12}	E_{21}	E_{22}
Intrinsic values	2.032	4.53	0.8	0	1.013	0.6	0.03	0	0	0.01
Inferred mean values	2.026	4.537	0.803	-0.014	1.054	0.596	0.029	-0.000	-0.000	0.010

Table I: Results from the inference of numerically simulated system (7). The first row describes the physical meaning of the parameters, the last two rows show the values of the intrinsic parameters and their inferred mean values, respectively. The results are presented for one window of data around $t = 1980$ s.

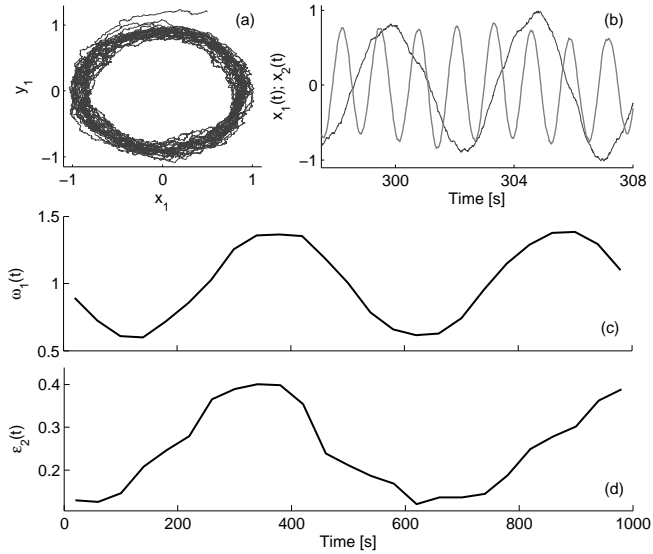


Figure 3: Inference of time-varying parameters from model of two coupled limit-cycle oscillators (8). Phase portrait showing the noisy state of the first oscillator (a). The time-series of the two oscillators $x_1(t)$ and $x_2(t)$ (b). The inferred time-evolution of the frequency parameter (c), and the net coupling from the first to the second oscillator (d).

reconstructed effectively. Because of the oscillatory nature and the periodic solutions, we decompose the phase dynamics in Fourier series. Hence, the Fourier series up to some order serve as base functions for the Bayesian inference. Care must be taken to ensure that the functions are not very linearly dependent, such as $\sin(x)$ and $\sin(-x)$, which can lead to imprecise and wrong separation of parameters within the inference. In the following, we used only one side of the expansion, e.g. for $\sin(n\phi_1 + m\phi_2)$ we used the components $n = 1, \dots, K$ instead of $n = -K, \dots, K$. The results for the reconstruction of the time-varying parameters are presented in Fig. 3 (c) and (d). The periodic sine variations are evident both in the frequency and the coupling strength. Note that the coupling amplitude is evaluated as a norm of all the relevant inferred parameters that describe this influence.

One can use the inferred parameters not only for evaluation of characteristics of individual oscillators, but also to determine if the coupled system undergoes some qualitative transitions. An obvious example of the latter is the detection of synchronization. For this reason we modify the parameters of model (8) with $\omega_1(t) = 1 - 0.4 \sin(2\pi 0.0022t)$, constant coupling parameter $\varepsilon_2 = 0.2$ and $\omega_2 = 1.4$. Such a constel-

lation of parameters takes the coupled system into and out of synchrony intermittently. The phase difference presented on Fig. 4 (a) is bounded during the synchronized intervals [20]. Applying the procedure of return maps and the modified Newton root-finding method [2] we detected the synchronization intervals (Fig. 4 (b)) consistently with the phase difference. The map procedure is equivalent to determining if a model of coupled phase oscillators, with parameters as the one inferred, is synchronized. Note also that during the synchronized intervals, the phases become almost identical and they do not span enough the available space for inference. This can result in inferred parameters that are far from the intrinsic values. However, the whole set of parameters is again correlated as if it was coming from a synchronized system. One might ask – why we need to construct such a ‘complicated’ procedure to detect synchronization, when something as simple as phase difference can give the similar answer. The point is that with the use of the intrinsic inferred parameters one can distinguish whether the phase slips and synchronization transitions are noise-induced or not [1].

Coupling functions are arguably the most important part of the description of interactions. They can describe the functional relationship, and the law governing the mutually interactions and the routes to qualitative transitions. Coupling functions have been used to describe different aspects of the interactions of oscillatory systems of various natures, including cardio-respiratory, electrochemical and mechanical

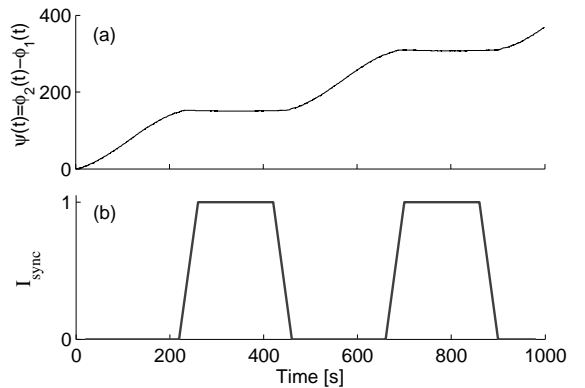


Figure 4: Detection of intermittent synchronization from system (8). Phase difference $\psi(t)$ showing the qualitative statistical occurrence of synchronized intervals – these appeared as bounded plateaus (a). Synchronization index demonstrating the detected intrinsic synchronization intervals (b), evaluated from the inferred parameters. High values $I_{sync} = 1$ denote the synchronized intervals.

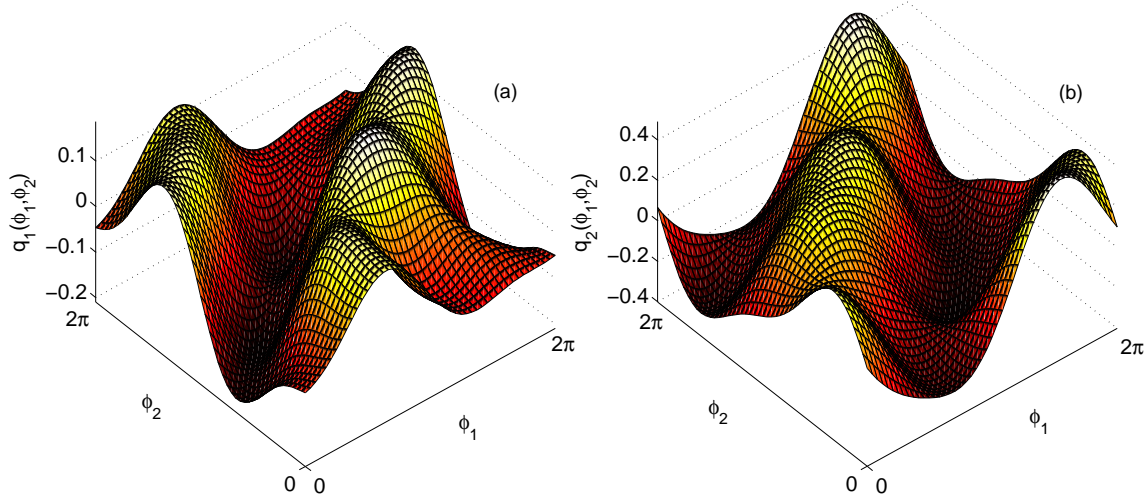


Figure 5: Coupling functions from the model of two interacting limit-cycle oscillators (8). The functional influence $q_1(\phi_1, \phi_2)$ from the second to the first oscillator is shown in (a); similarly the coupling function $q_2(\phi_1, \phi_2)$ from the first to the second oscillator is shown in (b). The functions are inferred within one window of data.

[1, 11–14, 22]. By representing the phase dynamics on a 2π -phase grid evaluated for the relevant inferred parameters, we can effectively determine and visualize them. The coupling functions of systems (8) for one window are shown in Fig. 5. By inferring the dynamics while allowing the time-variability to be traced, we can follow the actual time-evolution of the functions [1]. Moreover, the coupling function $q_i(\phi_i, \phi_j)$ can be further decomposed on self, direct and indirect coupling influences [23], and each one can be studied separately.

V. GENERALIZATIONS

The aim of the discussion in the previous sections was to present the implementation of the Bayesian inference in a clear and simple way. Needless to say, the framework is much broader and a number of important generalizations are possible.

The presentation mainly concentrated on the inference of phase dynamics. The main reason for this was to present a method that will be generally applicable to coupled oscillatory systems. However, there are many situations where the dynamics need to be analyzed directly from the measured signals in state space. For example, the estimation of the phases from chaotic systems can be problematic, while the inference in the state domain is not at all. If state signals are about to be analyzed, then Eq. (1) will have different type of base functions, e.g. polynomial, while all the rest of the equations and algorithms can be equally applied on the state signals. For examples of inference of (coupled) oscillatory dynamics in state space see [3–5].

The examples here included only two coupled systems, while in general the technique can be applied to larger group i.e. small-scale network of oscillators [2]. The phase decompositions can be applied for pairwise couplings but, more importantly, joint coupling influences can also be inferred. In

such cases, the effective coupling [24] can be distinguished from the structural by appropriate use of surrogate testing [25].

The procedure of information propagation that allows time-variability to be tracked, depends on p_w which acts as a free parameter. One can further improve this by making the parameter adaptive in order to follow the time-variability more closely and to infer the noise more precisely. This might be realized by determining the optimal parameter from a spectrum of values within each window. Even though this procedure will be very slow, it might prove helpful and needed in some cases.

Within the framework of the phase dynamics inference, the phase differential $\dot{\phi}_n$ is calculated as $\dot{\phi}_n = (\phi_{n+1} - \phi_n)/h$. Improved performance can be accomplished if one provides this as directly estimated instantaneous frequency – e.g. using synchrosqueezed [21] or nonlinear mode decomposition [26]. The phase base functions are not strictly restricted to be from the Fourier order decomposition, and other additional functions can be included. For example, if we have expansion up to second order $K = 2$, one can include also other components such as $\sin(7\phi_1 - 4\phi_2)$ in order to detect synchronization more precisely for 7:4 synchronization ratios.

VI. CONCLUDING REMARKS

We presented a tutorial intended to familiarize the reader with a technique for Bayesian inference of time-evolving coupled dynamics in the presence of noise. The tutorial gives a relatively comprehensive description of the method, including theoretical constraints, algorithms, implementation and demonstration of the main features on few characteristic examples. MatLab codes for the method and the examples are also available. This tutorial could lead the readers to new insights and little researched phenomena, promising to be a use-

ful tool for signal processing of a diverse nature.

[1] T. Stankovski, A. Duggento, P. V. E. McClintock, and A. Stefanovska, Phys. Rev. Lett. **109**, 024101 (2012).

[2] A. Duggento, T. Stankovski, P. V. E. McClintock, and A. Stefanovska, Phys. Rev. E **86**, 061126 (2012).

[3] D. G. Luchinsky, V. N. Smelyanskiy, A. Duggento, and P. V. E. McClintock, Phys. Rev. E **77**, 061105 (2008).

[4] A. Duggento, D. G. Luchinsky, V. N. Smelyanskiy, I. Kovanov, and P. V. E. McClintock, Phys. Rev. E **77**, 061106 (2008).

[5] V. N. Smelyanskiy, D. G. Luchinsky, A. Stefanovska, and P. V. E. McClintock, Phys. Rev. Lett. **94**, 098101 (2005).

[6] M. G. Rosenblum and A. S. Pikovsky, Phys. Rev. E **64**, 045202 (2001).

[7] M. Paluš and A. Stefanovska, Phys. Rev. E **67**, 055201(R) (2003).

[8] J. Jamšek, M. Paluš, and A. Stefanovska, Phys. Rev. E **81**, 036207 (2010).

[9] M. Staniek and K. Lehnertz, Phys. Rev. Lett. **100**, 158101 (2008).

[10] A. Bahraminasab, F. Ghasemi, A. Stefanovska, P. V. E. McClintock, and H. Kantz, Phys. Rev. Lett. **100**, 084101 (2008).

[11] B. Kralemann, L. Cimponeriu, M. Rosenblum, A. Pikovsky, and R. Mrowka, Phys. Rev. E **76**, 055201 (2007).

[12] I. T. Tokuda, S. Jain, I. Z. Kiss, and J. L. Hudson, Phys. Rev. Lett. **99**, 064101 (2007).

[13] J. Miyazaki and S. Kinoshita, Phys. Rev. Lett. **96**, 194101 (2006).

[14] I. Z. Kiss, Y. Zhai, and J. L. Hudson, Phys. Rev. Lett. **94**, 248301 (2005).

[15] P. Tass, M. G. Rosenblum, J. Weule, J. Kurths, A. Pikovsky, J. Volkmann, A. Schnitzler, and H.-J. Freund, Phys. Rev. Lett. **81**, 3291 (1998).

[16] F. Mormann, K. Lehnertz, P. David, and C. E. Elger, Physica D **144**, 358 (2000).

[17] B. Schelter, M. Winterhalder, R. Dahlhaus, J. Kurths, and J. Timmer, Phys. Rev. Lett. **96**, 208103 (2006).

[18] Y. Kuramoto, *Chemical Oscillations, Waves, and Turbulence* (Springer-Verlag, Berlin, 1984).

[19] B. Kralemann, L. Cimponeriu, M. Rosenblum, A. Pikovsky, and R. Mrowka, Phys. Rev. E **77**, 066205 (2008).

[20] A. Pikovsky, M. Rosenblum, and J. Kurths, *Synchronization – A Universal Concept in Nonlinear Sciences* (Cambridge University Press, Cambridge, 2001).

[21] I. Daubechies, J. Lu, and H. Wu, Appl. and Comput. Harmon. Anal. **30**, 243 (2011).

[22] R. F. Galán, G. B. Ermentrout, and N. N. Urban, Phys. Rev. Lett. **94**, 158101 (2005).

[23] D. Iatsenko, A. Bernjak1, T. Stankovski, Y. Shiogai, P. J. Owen-Lynch, P. B. M. Clarkson, P. V. E. McClintock, and A. Stefanovska, Phil. Trans. R. Soc. Lond. A, in press (2013).

[24] B. Kralemann, A. Pikovsky, and M. Rosenblum, Chaos **21**, 025104 (2011).

[25] T. Schreiber and A. Schmitz, Physica D **142**, 346 (2000).

[26] D. Iatsenko, A. Stefanovska, and P. V. E. McClintock, (submitted to Appl. Comp. Harm. Anal.) p. arXiv:1207.5567 [math.NA] (2012).

[27] One should also note that the inference is by definition stochastic, and inferring time-series without noise at all, will lead to singularities in Eqs. (3)-(6) and will stop the program. However, (a) for such noiseless case much simpler methods can be used e.g. least-squares fit, and (b) this situation is of very small use because it is (almost) never encounter in time-series from real measurements.

[28] www.lancs.ac.uk/depts/spc/research/nbmphysics/codesamples